

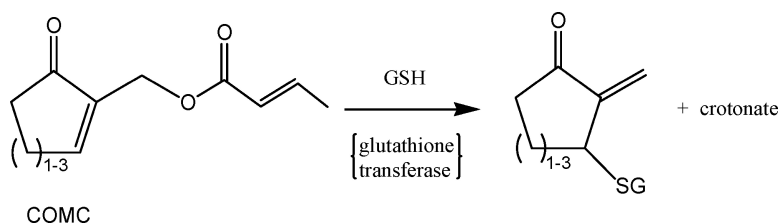
Article

## Mechanism of the Glutathione Transferase-Catalyzed Conversion of Antitumor 2-Crotonyloxymethyl-2-cycloalkenones to GSH Adducts

Diana S. Hamilton, Xiyun Zhang, Zhebo Ding, Ina Hubatsch, Bengt Mannervik, K. N. Houk, Bruce Ganem, and Donald J. Creighton

*J. Am. Chem. Soc.*, **2003**, 125 (49), 15049-15058 • DOI: 10.1021/ja030396p • Publication Date (Web): 12 November 2003

Downloaded from <http://pubs.acs.org> on March 30, 2009



### More About This Article

Additional resources and features associated with this article are available within the HTML version:

- Supporting Information
- Access to high resolution figures
- Links to articles and content related to this article
- Copyright permission to reproduce figures and/or text from this article

[View the Full Text HTML](#)



**ACS Publications**  
 High quality. High impact.

## Mechanism of the Glutathione Transferase-Catalyzed Conversion of Antitumor 2-Crotonyloxymethyl-2-cycloalkenones to GSH Adducts

Diana S. Hamilton,<sup>\*,†</sup> Xiyun Zhang,<sup>‡</sup> Zhebo Ding,<sup>‡</sup> Ina Hubatsch,<sup>§</sup> Bengt Mannervik,<sup>§</sup> K. N. Houk,<sup>‡</sup> Bruce Ganem,<sup>‡</sup> and Donald J. Creighton<sup>\*,†</sup>

Contribution from the Department of Chemistry and Biochemistry, University of Maryland Baltimore County, Baltimore, Maryland 21250, Department of Chemistry and Chemical Biology, Baker Laboratory, Cornell University, Ithaca, New York 14853-1301, Department of Chemistry and Biochemistry, University of California, Los Angeles, California 90095-1569, and Department of Biochemistry, Uppsala University, Biomedical Center, Box 576, SE-751 23 Uppsala, Sweden

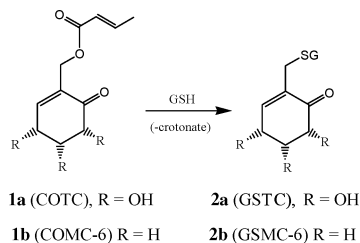
Received July 3, 2003; E-mail: hamilton@umbc.edu; creight@umbc.edu

**Abstract:** Human glutathione (GSH) transferase (hGSTP1-1) processes with similar kinetic efficiencies the antitumor agents 2-crotonyloxymethyl-2-cyclohexenone (COMC-6), 2-crotonyloxymethyl-2-cycloheptenone (COMC-7), and 2-crotonyloxymethyl-2-cyclopentenone (COMC-5) to 2-glutathionylmethyl-2-cyclohexenone, 2-glutathionylmethyl-3-glutathionyl-2-cycloheptenone, and 2-glutathionylmethyl-2-cyclopentenone, respectively. This process likely involves initial enzyme-catalyzed Michael addition of GSH to the COMC derivative to give a glutathionylated enol(ate), which undergoes nonstereospecific ketonization, either while bound to the active site or free in solution, to a glutathionylated exocyclic enone. Free in solution, GSH reacts at the exomethylene carbon of the exocyclic enone, displacing the first GSH to give the final product. This mechanism is supported by the observation of multiphasic kinetics in the presence of high concentrations of hGSTP1-1 and the ability to trap kinetically competent exocyclic enones in aqueous acid using COMC-6 and COMC-7 as substrates. That the exocyclic enone is formed by nonstereospecific ketonization of an enol(ate) species is indicated by the observation that COMC-6 (chirally labeled with deuterium at the exomethylene carbon) gives stereorandomly labeled exocyclic enone. The isozymes hGSTP1-1, hGSTA1-1, hGSTA4-4, and hGSTM2-2 catalyze the conversion of COMC-6 to final product with similar efficiencies ( $K_m = 0.08\text{--}0.34\text{ mM}$ ,  $k_{cat} = 1.5\text{--}6.1\text{ s}^{-1}$ ); no activity was detected with the rat rGSTT2-2 isozyme. Molecular docking studies indicate that in hGSTP1-1, the hydroxyl group of Tyr108 might serve as a general acid catalyst during substrate turnover. The possible significance of these observations with respect to the metabolism of COMC derivatives in multidrug resistant tumors is discussed.

### Introduction

Glutathione transferase (hGSTP1-1) has recently been reported to play a potentially important role in the metabolism of the antitumor agent 2-crotonyloxymethyl-2-cyclohexenone (COMC-6, **1b**).<sup>1,2</sup> This compound is a simple synthetic analogue<sup>3</sup> of 2-crotonyloxymethyl-(4*R*,5*R*,6*R*)-4,5,6-trihydroxy-2-cyclohexenone (COTC, **1a**), an antitumor metabolite first identified in *Streptomyces* in 1975 (Scheme 1).<sup>4</sup>

### Scheme 1



The antitumor activity of COTC was originally hypothesized to result from competitive inhibition of the methylglyoxal-de-toxifying enzyme glyoxalase I by the GSH adduct **2a**.<sup>4</sup> However, authentic samples of both **2a** and **2b** proved to be poor competitive inhibitors of human glyoxalase I,<sup>1,5</sup> with no significant antitumor activity in vitro.<sup>2</sup> Subsequently, the *pi* isozyme of human glutathione transferase (hGSTP1-1) was discovered to

<sup>†</sup> University of Maryland Baltimore County.

<sup>‡</sup> University of California, Los Angeles.

<sup>§</sup> Cornell University.

<sup>§</sup> Uppsala University.

- (1) Hamilton, D. S.; Ding, Z.; Ganem, B.; Creighton, D. J. *Org. Lett.* **2002**, *4*, 1209–1212.
- (2) Joseph, E.; Eiseman, J. L.; Hamilton, D. S.; Wang, H.; Tak, H.; Ganem, B.; Creighton, D. J. *J. Med. Chem.* **2003**, *46*, 194–196.
- (3) Aghil, O.; Bibby, M. C.; Carrington, S. J.; Double, J.; Douglas, K. T.; Phillips, R. M.; Shing, T. K. M. *Anti-Cancer Drug Des.* **1992**, *7*, 67–82.
- (4) (a) Takeuchi, T.; Chimura, H.; Hamada, M.; Umezawa, H.; Yoshioka, O.; Oguchi, N.; Takahashi, Y.; Matsuda, A. *J. Antibiot.* **1975**, *28*, 737–742. (b) Chimura, H.; Nakamura, H.; Takita, T.; Takeuchi, T.; Umezawa, H.; Kato, K.; Saito, S.; Tomisawa, T.; Iitaka, Y. *J. Antibiot.* **1975**, *28*, 743–748.

- (5) Huntley, C. F. M.; Hamilton, D. S.; Creighton, D. J.; Ganem, B. *Org. Lett.* **2000**, *2*, 3143–3144.

## Scheme 2

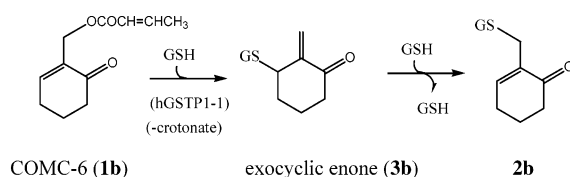
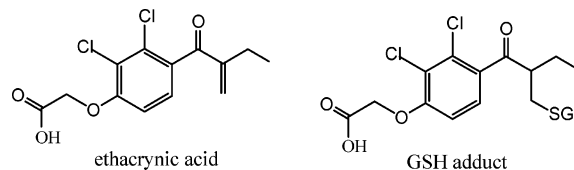


## Chart 1



catalyze the conjugation of GSH to COMC-6 (Scheme 1).<sup>1</sup> Preliminary kinetic studies and intermediate trapping experiments suggested that the minimum kinetic mechanism involved enzyme-catalyzed Michael addition of GSH to COMC-6 to give an electrophilic exocyclic enone (3b) that reacts with free GSH to give 2b (Scheme 2).

Thus, the antitumor activities of COTC and COMC-6 might reflect the reaction of the exocyclic enones with proteins and/or nucleic acids critical to cell viability.<sup>6</sup> From a pharmacological perspective, a substrate that is transformed to a toxic product by glutathione transferase (GST) is of considerable interest as a possible means of inhibiting multidrug-resistant tumors, which often overexpress specific isozymes of GST.<sup>7</sup>

To better understand the chemical mechanism of this process and to identify possible active-site residues involved in catalysis, the kinetic properties, reaction stereochemistry, and isozyme specificities of COMC-6 and its five- and seven-membered-ring homologues have been determined. The results of these studies, together with molecular docking experiments, suggest that the COMC derivatives are processed by a mechanism analogous to that for the GST-catalyzed addition of GSH to the enone ethacrynic acid (Chart 1).

## Experimental Section

**Materials.** Deuterated reagents, *R*-( $-$ )- $\alpha$ -methoxy- $\alpha$ -trifluoromethylphenyl acid chloride (*R*-MTPA chloride), human placental GST (predominantly the hGSTP1-1 isoform), recombinant hGSTP1-1, and horse liver alcohol dehydrogenase (HLADH) were purchased from Sigma-Aldrich Chemical Co. Salts and free GSH were removed from human placental GST by ultrafiltration prior to use. The isolation and purification of other recombinant isoforms of GST used in this study have been described elsewhere.<sup>8</sup>

**Synthesis of COMC Derivatives.** The synthesis of the 2-crotonyl-oxymethyl-2-cycloalkenones 1b–d utilized the known Baylis–Hillman reaction of commercially available 2-cycloalkenones 4b–d with formaldehyde to prepare the 2-hydroxymethyl-2-cycloalkenones 5b–d,<sup>9</sup> which were then treated with crotonic anhydride<sup>3</sup> to give 1b–d (Scheme 3).

Detailed descriptions of the preparation of 1b–d have been published.<sup>1,2</sup> The GSH conjugates 2b<sup>1</sup>, 2c, and 2d were prepared by separately incubating 1b (26 mM), 1c (117 mM), and 1d (64 mM) with equimolar concentrations of GSH in phosphate buffer at pH 7.4 (37 °C) for 20 min, 40 and 48 h, respectively. The crude products were purified by anion-exchange chromatography (Dowex-1).<sup>5</sup>

**2-Glutathionylmethyl-2-cyclohexenone (2b).** (Yield 99%). 300 MHz <sup>1</sup>H NMR (D<sub>2</sub>O):  $\delta$  7.13 (t, *J* = 4.3 Hz, vinyl H), 4.50 (q, *J* = 4.8, 8.6 Hz, Cys-C $\alpha$ H), 3.95 (s, Gly-C $\alpha$ H<sub>2</sub>), 3.94 (t, *J* = 6.4 Hz, Glu-C $\alpha$ H), 3.26 (s, CH<sub>2</sub>), 2.93 (q, *J* = 4.8, 14.5 Hz, Cys-C $\beta$ H<sub>a</sub>), 2.75 (q, *J* = 8.6, 14.5 Hz, Cys-C $\beta$ H<sub>b</sub>), 2.51 (m, Glu-C $\gamma$ H<sub>2</sub>), 2.45–2.38 (m, ring CH<sub>2</sub>), 2.16 (m, Glu-C $\beta$ H<sub>2</sub>), 1.98–1.92 (m, ring CH<sub>2</sub>). <sup>13</sup>C NMR (D<sub>2</sub>O):  $\delta$  203.3, 176.6, 174.4, 172.9, 172.7, 153.0, 134.2, 52.9, 52.7, 41.1, 37.8, 32.5, 30.9, 30.0, 25.7, 25.6, 22.2. ESI-MS *m/z* 416 (M + 1, 100%): 287 (9%).

**2-Glutathionylmethyl-2-cyclopentenone (2c).** (Yield 83%). 300 MHz <sup>1</sup>H NMR (D<sub>2</sub>O, HOD ref):  $\delta$  6.92 (m, vinyl H), 4.52 (q, *J* = 4.8, 8.4 Hz, Cys-C $\alpha$ H), 3.95 (s, Gly-C $\alpha$ H<sub>2</sub>), 3.80 (t, *J* = 6.4 Hz, Glu-C $\alpha$ H), 3.33 (s, CH<sub>2</sub>), 2.96 (q, *J* = 4.8, 13.9 Hz, Cys-C $\beta$ H<sub>a</sub>), 2.78 (q, *J* = 8.4, 13.9 Hz, Cys-C $\beta$ H<sub>b</sub>), 2.66 (m, ring CH<sub>2</sub>), 2.53–2.45 (m, Glu-C $\gamma$ H<sub>2</sub>, ring CH<sub>2</sub>), 2.14 (m, Glu-C $\beta$ H<sub>2</sub>). <sup>13</sup>C NMR (D<sub>2</sub>O):  $\delta$  211.5, 173.9, 171.9, 170.4, 169.9, 163.3, 137.8, 50.7, 50.1, 38.5, 32.2, 29.8, 28.4, 24.2, 23.2, 22.1, 17.6. ESI-MS *m/z* 402 (M + 1, 100%): 273 (18%).

**2-Glutathionylmethyl-2-cycloheptenone (2d).** (Yield 38%). 300 MHz <sup>1</sup>H NMR (D<sub>2</sub>O, HOD ref):  $\delta$  7.80 (t, *J* = 6.3 Hz, vinyl H), 4.52 (q, *J* = 4.8, 8.4 Hz, Cys-C $\alpha$ H), 3.97 (s, Gly-C $\alpha$ H<sub>2</sub>), 3.90 (t, *J* = 6.2 Hz, Glu-C $\alpha$ H), 3.35 (s, CH<sub>2</sub>), 2.96 (q, *J* = 5.1, 13.9 Hz, Cys-C $\beta$ H<sub>a</sub>), 2.77 (q, *J* = 8.8, 13.9 Hz, Cys-C $\beta$ H<sub>b</sub>), 2.60 (m, ring CH<sub>2</sub>), 2.56–2.43 (m, Glu-C $\gamma$ H<sub>2</sub>, ring CH<sub>2</sub>), 2.17 (m, Glu-C $\beta$ H<sub>2</sub>), 1.76–1.68 (m, ring 2CH<sub>2</sub>). <sup>13</sup>C NMR (D<sub>2</sub>O):  $\delta$  206.1, 171.8, 170.2, 170.0, 146.9, 135.1, 113.1, 111.8, 58.8, 50.3, 50.2, 39.7, 38.4, 30.7, 29.6, 28.3, 24.6, 23.0, 21.6, 18.1. ESI-MS *m/z* 430 (M + 1, 100%): 402 (34%), 102 (67%).

**Synthesis of Chiral Deuterium-Labeled COMC Derivatives.** The deuterium-labeled substrates (*R*)d<sub>1</sub>-1b and (*S*)d<sub>3</sub>-1b were prepared by using HLADH to stereospecifically introduce different isotopes of hydrogen at the pro-*R* position of the exomethylene function of 5b, followed by crotonylation of the labeled alcohol. Thus, (*R*)d<sub>1</sub>-1b was prepared as outlined in Scheme 4.

The stereoisomer (*S*)d<sub>3</sub>-1b, in which the configuration at the deuterium labeled exomethylene carbon is *S*, was synthesized by the same procedure, using d<sub>4</sub>-5b and ethanol as starting materials. Compound d<sub>4</sub>-5b was prepared by electrophilic addition of dideuterioformaldehyde (in D<sub>2</sub>O) to cyclohexenone following a literature procedure.<sup>9</sup> Under the reaction conditions, the C6 methylene undergoes complete deuterium exchange with solvent.

Progress of the hydrogen-exchange reactions was followed by monitoring the time-dependent change in the integrated intensities of the exomethylene protons of substrates. Incubation times of two to four weeks, in the presence of 80 units of HLADH (pH 7, 20 °C), were required to effect >25% isotope exchange. No detectable exchange was observed in the absence of HLADH. This enzyme is known to catalyze stereospecific hydrogen transfer between the pro-*R* hydrogen of primary alcohols and C4 of the nicotinamide ring of NAD, as reviewed elsewhere.<sup>10</sup> Therefore, alcohol 5b was predicted to be stereospecifically processed by HLADH.

**Stereochemical Analysis.** The stereospecificities of the HLADH-catalyzed exchange reactions were verified by <sup>1</sup>H NMR spectroscopy of diastereomeric derivatives of the deuterium labeled products. First, the product mixtures used to prepare (*R*)d<sub>1</sub>-5b and (*S*)d<sub>3</sub>-5b were converted to the esters of the (*S*)-(-) enantiomer of Mosher's acid ( $\alpha$ -methoxy- $\alpha$ -trifluoromethylphenylacetic acid, MTPA) using the method of Ward and Rhee.<sup>11</sup> In CDCl<sub>3</sub>, the diastereotopic exomethylene protons of unlabeled 5b are observed as an AB quartet at  $\delta$  = 4.972 and 4.954.

(10) (a) Creighton, D. J.; Murthy, N. S. R. K. *The Enzymes* **1990**, *19*, 324–421. (b) Hummel, W. *Trends Biotechnol.* **1999**, *17*, 487–492.

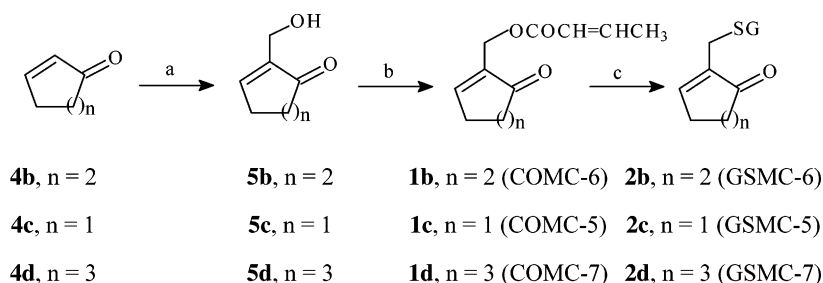
(11) Ward, D. E.; Rhee, C. K. *Tetrahedron Lett.* **1991**, *32*, 7165–7166.

(6) Zhang, Q.; Ding, Z.; Creighton, D. J.; Ganem, B.; Fabris, D. *Org. Lett.* **2002**, *4*, 1459–1462.

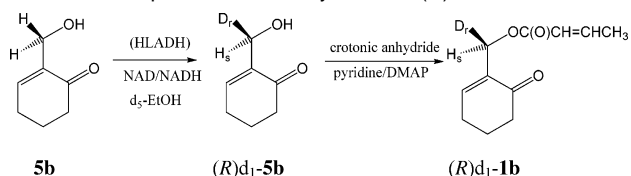
(7) Hayes, J. D.; Pulford, D. J. *Crit. Rev. Biochem. Mol. Biol.* **1995**, *30*, 445–600.

(8) (a) Stenberg, G.; Björnstedt, R.; Mannervik, B. *Protein Expression Purif.* **1992**, *3*, 80–84. (b) Hubatsch, I.; Ridderström, M.; Mannervik, B. *Biochem. J.* **1998**, *330*, 175–179. (c) Kolm, R. H.; Stenberg, G.; Widersten, M.; Mannervik, B. *Protein Expression Purif.* **1995**, *6*, 265–271. (d) Johansson, A.-S.; Bolton-Grob, R.; Mannervik, B. *Protein Expression Purif.* **1999**, *17*, 105–112. (e) Jemth, P.; Stenberg, G.; Chaga, G.; Mannervik, B. *Biochem. J.* **1996**, *316*, 131–136.

(9) Rezgui, F.; El Gaid, M. M. *Tetrahedron Lett.* **1998**, *39*, 5965–5966.

**Scheme 3.** Synthetic Route to COMC Derivatives and Their GSH Adducts<sup>a</sup>

<sup>a</sup> (a) DMAP, CH<sub>2</sub>O, THF, rt. (b) Crotonic anhydride, pyridine, DMAP, rt. (c) GSH, phosphate buffer (pH 7.4), 37 °C.

**Scheme 4.** Preparation of Chirally Labeled (*R*)d<sub>1</sub>-1b

The upfield and downfield resonances are assumed to correspond to the pro-*S* and pro-*R* protons, respectively, on the basis of chemical shift comparisons with MTPA esters of known configuration.<sup>12</sup> The <sup>1</sup>H NMR spectrum of the MTPA ester of the product mixture (composed of 50% **5b** and 50% (*R*)d<sub>1</sub>-**5b**), obtained by the method of Scheme 4, shows a quartet characteristic of **5b** and a singlet ( $\delta = 4.929$ ) corresponding to (*R*)d<sub>1</sub>-**5b**, indicating an isotope shift for the H<sub>s</sub> proton of 0.025 ppm (Figure 1a). The <sup>1</sup>H NMR spectrum of the MTPA ester of the product mixture containing (*S*)d<sub>3</sub>-**5b** shows a singlet at  $\delta = 4.958$ , indicating an isotope shift for the H<sub>r</sub> proton of 0.014 ppm (Figure 1b). These spectra are similar to those of the (*S*)-MTPA esters of pro-*R* and pro-*S* D-labeled benzyl alcohols.<sup>12b</sup> The NMR spectra of Figure 1 indicate that (*S*)d<sub>3</sub>-**5b** and (*R*)d<sub>1</sub>-**5b** are isomerically pure, and therefore crotonylation of these compounds will give isomerically pure (*S*)d<sub>3</sub>-**1b** and (*R*)d<sub>1</sub>-**1b**.

**2-(*R*)-Deuteriohydroxymethyl-2-cyclohexenone ((*R*)d<sub>1</sub>-**5b**):** prepared by incubating **5b** (3.6 mmol, 50 mM), HLADH (80 U), NAD (10 mM) and d<sub>3</sub>-ethanol (250 mM) for 12 days in 0.1 M HEPES, pH 7.2, 20 °C. The reaction mixture was diluted with brine and extracted with 3 portions of dichloromethane in the presence of a small amount of sodium dodecyl sulfate to break the emulsion. The combined organic layers were washed with water and dried over sodium sulfate, and the solvent was removed in vacuo to give a colorless liquid which yellowed slightly on standing. (Yield 75%). <sup>1</sup>H NMR analysis indicated that the product was composed of an approximate 1:1 mixture of **5b** and d<sub>1</sub>-**5b**, on the basis of the 25% decrease in the integrated intensity of the hydroxymethylene proton resonance ( $\delta$  4.24). For the product mixture: 300 MHz <sup>1</sup>H NMR (CDCl<sub>3</sub>, TMS):  $\delta$  6.94 (t,  $J = 4.0$  Hz, vinyl H), 4.24 (s, 1.5 H, exocyclic CH<sub>2</sub> and CHD), 2.53–2.38 (m, ring 2CH<sub>2</sub>), 2.06–1.98 (m, ring CH<sub>2</sub>), 1.61 (s, OH).

**2-Dideuteriohydroxymethyl-6,6-dideuterio-2-cyclohexenone (d<sub>4</sub>-**5b**):** prepared by reacting **4b** with a commercial preparation of dideuterioformaldehyde (supplied in D<sub>2</sub>O) under the conditions used to prepare **5b**.<sup>9</sup> Under these conditions, complete deuterium exchange occurs with the methylene protons at C6, as these resonances are absent from the <sup>1</sup>H NMR spectrum. (Yield 18%). 300 MHz <sup>1</sup>H NMR (CDCl<sub>3</sub>, TMS):  $\delta$  6.95 (t,  $J = 4.2$  Hz, vinyl H), 2.44–2.38 (m, ring CH<sub>2</sub>), 2.01 (t,  $J = 5.7$  Hz, ring CH<sub>2</sub>), 1.64 (s, OH).

**(*S*)-2-Deuteriohydroxymethyl-6,6-dideuterio-2-cyclohexenone ((*S*)d<sub>3</sub>-**5b**):** prepared by incubating d<sub>4</sub>-**5b** (3.6 mmol, 50 mM), HLADH (80 U), NAD (10 mM), and ethanol (250 mM) for 35 days in 0.1 M HEPES pH 7.2, 20 °C. The reaction mixture was worked up by the

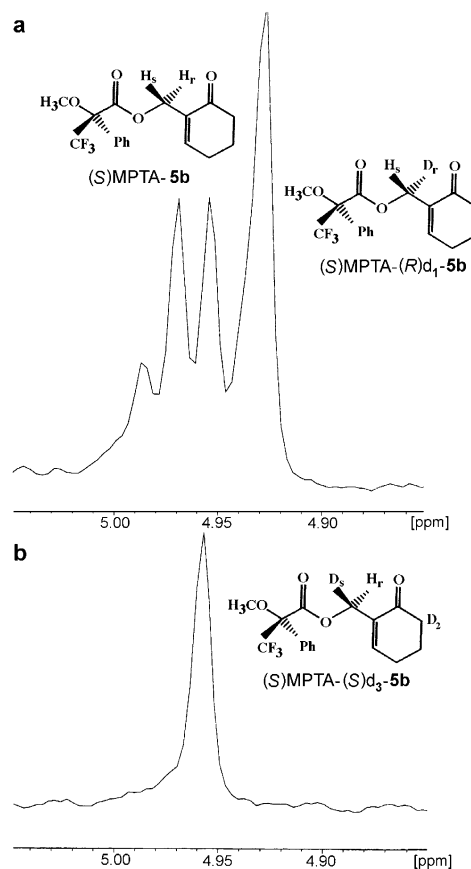


**Figure 1.** Exomethylene region in the <sup>1</sup>H NMR spectra (800 MHz, CDCl<sub>3</sub>/TMS) of the Mosher's esters of the product mixture (a) containing 50% **5b** and 50% (*R*)d<sub>1</sub>-**5b** and (b) (*S*)d<sub>3</sub>-**5b**.

same procedure used to prepare (*R*)d<sub>1</sub>-**5d** to give a colorless liquid. (Yield 80%). <sup>1</sup>H NMR analysis indicated that the product was composed of an approximate 1:1 mixture of d<sub>4</sub>-**5b** and d<sub>3</sub>-**5b**, on the basis of the integrated intensity of the hydroxymethylene proton resonance ( $\delta$  4.24). 300 MHz <sup>1</sup>H NMR (CDCl<sub>3</sub>, TMS):  $\delta$  6.94 (t,  $J = 4.0$  Hz, vinyl H), 4.22 (s, 0.5 H, exocyclic CD<sub>2</sub> and CHD), 2.44–2.38 (m, ring CH<sub>2</sub>), 2.01 (t,  $J = 5.7$  Hz, ring CH<sub>2</sub>), 1.62 (s, OH).

**(*R*)-2-Crotonyloxydeuteriomethyl-2-cyclohexenone ((*R*)d<sub>1</sub>-**1b**):** prepared by treating the (*R*)d<sub>1</sub>-**5b**/**5b** mixture, obtained as described above, with crotonic anhydride<sup>3</sup> to give a colorless liquid. (Yield 69%). 300 MHz <sup>1</sup>H NMR (CDCl<sub>3</sub>, TMS):  $\delta$  7.04–6.94 (m, 2 vinyl H), 5.86 (d,  $J = 15.4$  Hz, vinyl H), 4.81 (s, ~1.5 H, exocyclic CH<sub>2</sub> and CHD), 2.49–2.39 (m, ring 2CH<sub>2</sub>), 2.06–1.98 (m, ring CH<sub>2</sub>), 1.90 (d,  $J = 7.0$  Hz, CH<sub>3</sub>).

**(*S*)-2-Crotonyloxydeuteriomethyl-6,6-dideuterio-2-cyclohexenone ((*S*)d<sub>3</sub>-**1b**):** prepared by treating the d<sub>4</sub>-**5b**/**(S)**d<sub>3</sub>-**5b** mixture, obtained as described above, with crotonic anhydride<sup>3</sup> to give a colorless liquid. (Yield 59%). 300 MHz <sup>1</sup>H NMR (CDCl<sub>3</sub>, TMS):  $\delta$  7.04–6.94

(12) (a) Dale, J. A.; Mosher, H. S. *J. Am. Chem. Soc.* **1973**, *95*, 512. (b) Wolfe, S.; Yang, K.; Weinberg, N.; Shi, Z.; Hsieh, Y.-H.; Sharma, R. D.; Ro, S.; Kim, C.-K. *Chem.-Eur. J.* **1998**, *4*, 886–902.

(m, 2 vinyl H), 5.86 (dq,  $J = 2.6, 15.8$  Hz, vinyl H), 4.79 (s,  $\sim 0.5$  H, exocyclic CD<sub>2</sub> and CHD), 2.49–2.39 (m, ring CH<sub>2</sub>), 2.05–1.99 (m, ring CH<sub>2</sub>), 1.86 (dd,  $J = 1.8, 7.0$  Hz, CH<sub>3</sub>).

**Kinetic Measurements.** For each conjugation reaction, kinetic measurements were carried out near a wavelength of maximum difference absorbency of products minus reactants: COMC-6 (**1b**),  $\Delta\epsilon_{235} -2400$  cm<sup>-1</sup> M<sup>-1</sup>; COMC-5 (**1c**),  $\Delta\epsilon_{225} -6600$  cm<sup>-1</sup> M<sup>-1</sup> or  $\Delta\epsilon_{243} +1600$  cm<sup>-1</sup> M<sup>-1</sup>; and COMC-7 (**1d**),  $\Delta\epsilon_{235} -3500$  cm<sup>-1</sup> M<sup>-1</sup>. The kinetic constants associated with the GST-catalyzed conjugation of GSH with **1b–d** were obtained from reciprocal plots of initial rates ( $\Delta OD/\text{min}$ ) versus [substrate], pH 6.5, [GSH] = 1 mM (25 °C), under conditions where the enzyme-catalyzed step is rate limiting ( $< 0.08$  units GST in the assay cuvette). Units of GST activity were defined using 1-chloro-2,4-dinitrobenzene (CDNB) as substrate. Kinetic constants for different recombinant GSTs were obtained by curve-fitting the Michaelis–Menten equation to the initial rate data.

**Molecular Docking.** The structures of ethacrynic acid (EA), the GS–EA adduct, COMC-6 (**1b**), and the enolates formed from the addition of GSH to COMC-6 were optimized using MM3 or AMBER force fields in MacroModel 7.1.<sup>13</sup> HF/6-31G\* charges were assigned to atoms of all of the structures, and the program AutoDock<sup>14</sup> was used to predict preferred binding modes. The X-ray crystal structures of hGSTP1-1 in complex with EA or with GS–EA (PDB codes 2GSS and 3GSS, respectively) were used in docking simulations after removing all crystallographic water molecules and EA or GS–EA from the active sites. The Lamarckian genetic algorithm was used in certain AutoDock calculations.<sup>14</sup> One hundred twenty simulations were performed for each system. Each simulation was composed of a maximum of 500 000 energy evaluations and a maximum of 50 000 generations. Both rigid docking (deleting all rotatable torsion angles) and flexible docking (allowing all rotatable torsion angles) were applied.

## Results

**Kinetic Studies.** The antitumor activity of COMC-6 (**1b**) has been proposed to arise from a reactive exocyclic enone (**3b**) formed during the conjugation reaction between intracellular GSH and COMC-6 (Scheme 2).<sup>1</sup> Most recently, the five- and seven-membered-ring homologues (COMC-5 (**1c**) and COMC-7 (**1d**)) were also found to be potent inhibitors of B-16 melanotic melanoma in vitro with IC<sub>50</sub> values (144 and 29 nM, respectively) similar to that of COMC-6 (46 nM).<sup>2</sup> To test whether the antitumor activities of the homologues could be explained on the same basis as that of COMC-6, the kinetic properties of all three compounds, either in the presence or in the absence of human placental GST (predominantly the hGSTP1-1 isoform), were compared. The placental and recombinant hGSTP1-1 enzyme preparations gave identical kinetic constants with the COMC derivatives.

In the absence of hGSTP1-1, the reaction of COMC-6 with excess GSH follows a first-order decay, showing no evidence of an intermediate species (Figure 2).

However, in the presence of placental hGSTP1-1 the reaction rate profile conforms to a double exponential decay (Figure 3). The magnitude of the rate constant associated with the initial downward phase, after subtracting the rate constant for the nonenzymatic addition of GSH with COMC-6, is linearly dependent on the concentration of hGSTP1-1 in the range 0 to 2.4 (CDNB) units of enzyme activity. The magnitude of the

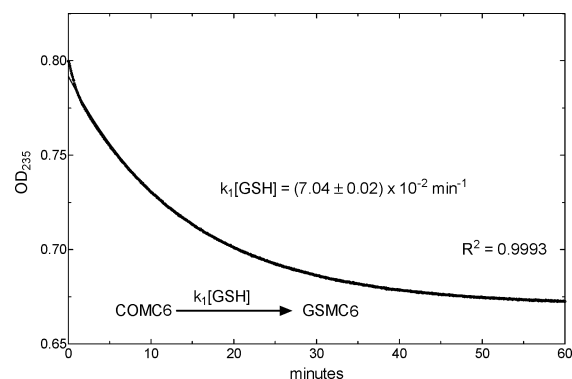


**Figure 2.** Rate profile for the reaction of COMC-6 (0.05 mM) with GSH (1.03 mM). Conditions: Potassium phosphate buffer (0.1 M, pH 6.5), EDTA (0.05 mM), 25 °C.

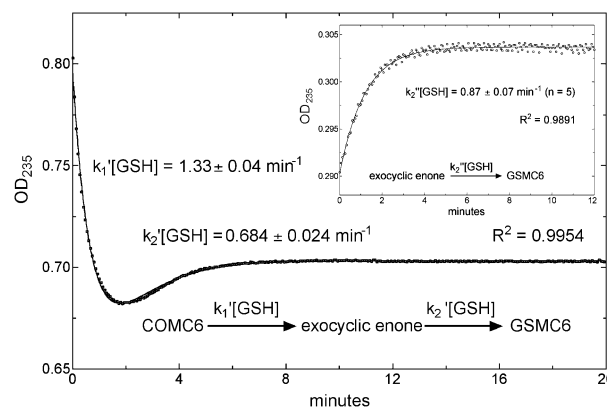


**Figure 3.** Rate profile for the reaction of COMC-6 (0.05 mM) with GSH (1.03 mM) in the presence of placental hGSTP1-1 (2.4 CDNB units). Rate constants were obtained as best-fit values to the equation  $OD_{235} = OD_{235(t=\infty)} + a(\exp(-k_1 t)) + b(\exp(k_2 t))$ . The inset shows the exponential rise in  $OD_{235}$  due to the reaction of the isolated exocyclic enone with GSH (1.04 mM). Conditions: Potassium phosphate buffer (0.1 M, pH 6.5), EDTA (0.05 mM), 25 °C.

rate constant associated with the second, upward phase of the reaction is independent of enzyme concentration.

These observations are consistent with enzyme-catalyzed formation of a reactive species that subsequently dissociates from the enzyme and reacts with GSH in bulk solvent to give GSMC-6. Brief incubation of COMC-6, GSH, and high concentrations of recombinant hGSTP1-1 gave rise to a transient species that was isolated by reverse-phase HPLC and confirmed to be an exocyclic enone by NMR spectroscopy.<sup>1</sup> Incubation of the exocyclic enone with GSH gave a species that co-migrated with authentic GSMC-6 during HPLC. Moreover, the spectrophotometrically determined pseudo-first-order rate constant for reaction of the exocyclic enone with GSH under the same buffer conditions was similar in magnitude to the second phase of the reaction of COMC-6 with GSH in the presence of hGSTP1-1 (Figure 3, inset). The absorptivity of the exocyclic enone ( $\epsilon = 4300$  cm<sup>-1</sup> M<sup>-1</sup>) was significantly less than that of GSMC-6 ( $\epsilon = 7500$  cm<sup>-1</sup> M<sup>-1</sup>), which accounts for the overall shape of the reaction rate profile in the presence of hGSTP1-1.

The five-membered-ring compound COMC-5 (**1c**) displayed biphasic kinetic properties similar to those of COMC-6 (data not shown). In the absence of hGSTP1-1, the reaction of excess GSH with COMC-5 followed a simple first-order decay, but in the presence of high concentrations of placental hGSTP1-1 the reaction rate profile conformed to a double exponential function.

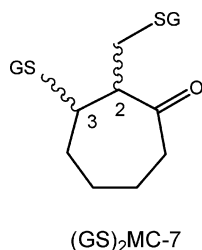
(13) Mohamadi, F.; Richard, N. G. J.; Liskamp, W. C.; Lipton, M.; Canfield, C.; Chang, G.; Hendrickson, T.; Still, W. C. *J. Comput. Chem.* **1990**, *11*, 440.

(14) Morris, G. M.; Goodsell, D. S.; Halliday, R. S.; Huey, R.; Hart, W. E.; Belew, R. K.; Olson, A. J. *J. Comput. Chem.* **1998**, *19*, 1639–1662.

As with COMC-6, the magnitude of the rate constant associated with the initial downward phase, after subtracting the rate constant associated for the nonenzymatic addition of GSH to COMC-5, was linearly dependent on the concentration of hGSTP1-1 in the range 0 to 1.0 CDNB units of enzyme activity. As for COMC-6, the magnitude of the rate constant associated with the second, upward phase of the reaction was independent of enzyme concentration. These observations are consistent with the formation of an exocyclic enone that dissociates from the enzyme and subsequently reacts with GSH in bulk solvent to give GSMC-5 (**2c**). Brief incubation of COMC-5, GSH, and recombinant hGSTP1-1 gave rise to a transient species that was partially purified by reverse-phase HPLC (8% aqueous methanol with 0.25% acetic acid). Incubation of this species with GSH in buffered solution gave a species that co-migrated with authentic GSMC-5 by HPLC. However, the instability of the transient species precluded the isolation of enough material for reliable kinetic and NMR characterization. Therefore, this intermediate could not be confirmed to be an exocyclic enone.

The reactions of the seven-membered-ring compound COMC-7 (**1d**) with GSH are more complex. In the absence of hGSTP1-1, the reaction of COMC-7 with excess GSH in aqueous buffer was best fit using a two-phase exponential decay, implying at least two sequential reactions (Figure 4).

As a function of time, aliquots from the reaction mixture were analyzed by reverse-phase HPLC (Waters  $\mu$ Bondapak C<sub>18</sub>, 7.8 mm i.d.  $\times$  30 cm, 10  $\mu$ m) using aqueous 20% methanol containing 0.25% acetic acid, as an eluting solvent. The initial phase of the reaction was characterized by the progressive increase in the intensity of a new peak that co-migrated with authentic GSMC-7 (**2d**, 21 min). At long incubation times this peak progressively decreased in intensity with a corresponding increase in the intensities of at least three different species with retention times of 12, 13, and 14 min. ESI FAB MS showed that each species gave identical molecular ions ( $M + Na^+ = 760$ ), consistent with the following structure:



Therefore, the product species are probably different diastereomers of the diglutathione adduct ( $GS$ )<sub>2</sub>MC-7, which differ with respect to the configurations at C2 and C3.

The progress curve for the reaction of COMC-7 with GSH in the presence of high concentrations of placental hGSTP1-1 could be fit with a triple exponential function (Figure 5).

The magnitude of the observed rate constant for the initial, rapid phase (after subtracting the rate constant for the nonenzymatic reaction) is linearly dependent on enzyme concentration from 0.1 to 1.0 CDNB units of placental hGSTP1-1. The rate constant  $k_2'$  appears to be associated with the conversion of the exocyclic enone to GSMC-7. Indeed, brief incubation of COMC-7, GSH, and recombinant hGSTP1-1 gave rise to a transient species that was isolated by reverse-phase HPLC, with a retention time (26 min) close to that of GSMC-7 (21 min). <sup>1</sup>H

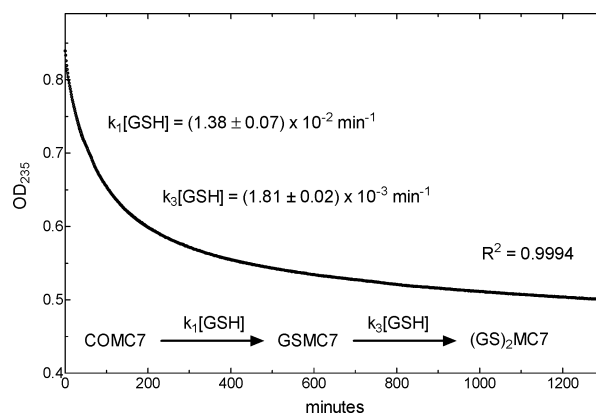


**Figure 4.** Rate profile for the reaction of COMC-7 (**1d**, 0.05 mM) with GSH (0.99 mM). The rate constants were obtained as best-fit values to the equation  $OD_{235} = OD_{235(t=\infty)} + a(\exp(-k_1t)) + b(\exp(-k_3t))$ . Conditions: Potassium phosphate buffer (0.1 M, pH 6.5), EDTA (0.05 mM), 1% ethanol, 25 °C.

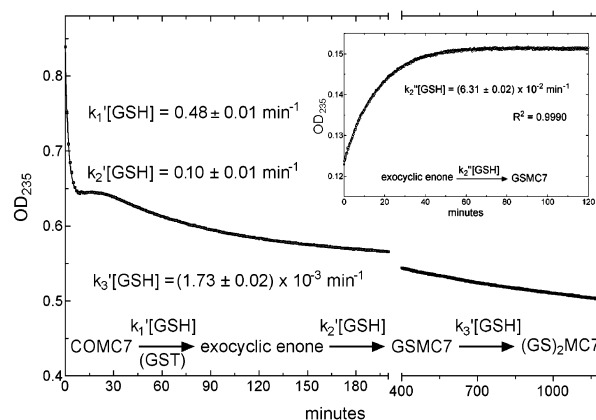


**Figure 5.** Rate profile for the reaction of COMC-7 (**1d**, 0.05 mM) with GSH (1.05 mM), in the presence of human placental hGSTP1-1 (1 CDNB unit). The rate constants given in the figure are best-fit values to the equation  $OD_{235} = OD_{235(t=\infty)} + a(\exp(-k_1't)) + b(\exp(-k_2't)) + c(\exp(-k_3't))$ . The inset shows the exponential rise in  $OD_{235}$  due to the reaction of the isolated exocyclic enone with GSH (0.99 mM). Conditions: Potassium phosphate buffer (0.1 M, pH 6.5), EDTA (0.05 mM), 5% ethanol, 25 °C.

NMR spectroscopy confirmed the identity of an exocyclic enone. Incubation of this species with GSH in buffered solution gave a species that co-migrates with authentic GSMC-7 by HPLC. Moreover, the spectrophotometrically determined pseudo-first-order rate constant for the reaction of the exocyclic enone ( $\epsilon = 3200 \text{ cm}^{-1} \text{ M}^{-1}$ ) with GSH to give GSMC-7 ( $\epsilon = 5000 \text{ cm}^{-1} \text{ M}^{-1}$ ) was similar in magnitude to the second phase of the reaction of COMC-7 with GSH in the presence of hGSTP1-1 (Figure 5, inset). The slow decrease in absorbance with a rate constant  $k_3'[GSH]$  corresponds closely to  $k_3[GSH]$  for conversion of GSMC-7 to the diglutathione adduct ( $GS$ )<sub>2</sub>MC-7 in the absence of hGSTP1-1 (Figure 4).

A summary of the nonenzymatic kinetic constants is given in Table 1.

Under conditions where the enzyme-catalyzed step is rate-limiting ( $<0.08$  CDNB units GST), the rate constants for enzyme-catalyzed conjugation of GSH with the three different COMC derivatives were determined and compared with those for the uncatalyzed conjugation reaction obtained under the same buffer conditions (Table 2).

**Stereochemistry Studies.** To determine the stereochemistry of the conversion of COMC-6 to the exocyclic enone, COMC-6

**Table 1.** Comparison of the Second-Order Rate Constants for Reaction of GSH with Different COMC Derivatives ( $k_1$ ) and with the Corresponding Exocyclic Enones ( $k_2$ )<sup>a</sup>

derivative	$k_1$ , mM <sup>-1</sup> min <sup>-1</sup> (n)	$k_2$ , mM <sup>-1</sup> min <sup>-1</sup> (n)
COMC-5	0.102 ± 0.006 (5)	nd <sup>b</sup>
COMC-6	0.067 ± 0.003 (5)	0.861 ± 0.042 (4)
COMC-7	0.015 ± 0.002 (5)	0.063 ± 0.006 (7)

<sup>a</sup> Conditions: COMC-X (~0.05 mM), GSH (~1.0 mM), potassium phosphate buffer (0.1 M), pH 6.5, EDTA (0.05 mM), ethanol (0–5%), 25 °C. <sup>b</sup> nd, not determined.

**Table 2.** Kinetic Constants for the Human Placental HGSTP1-1 Catalyzed Conjugation of GSH with Different COMC Derivatives<sup>a</sup>

compound	$K_m$ , mM	$k_{cat}$ , min <sup>-1</sup>	$(k_{cat}/K_m) \times 10^{-3}$ , min <sup>-1</sup> mM <sup>-1</sup>
COMC-5	0.07 ± 0.02	70 ± 20	1.0 ± 0.4
COMC-6	0.05 ± 0.01	70 ± 20	1.4 ± 0.4
COMC-7	0.18 ± 0.02	180 ± 50	1.0 ± 0.3

<sup>a</sup> Conditions: COMC-X (~0.05 mM), GSH (~1.0 mM), potassium phosphate buffer (0.1 M), pH 6.5, EDTA (0.05 mM), ethanol (0–5%), 25 °C.

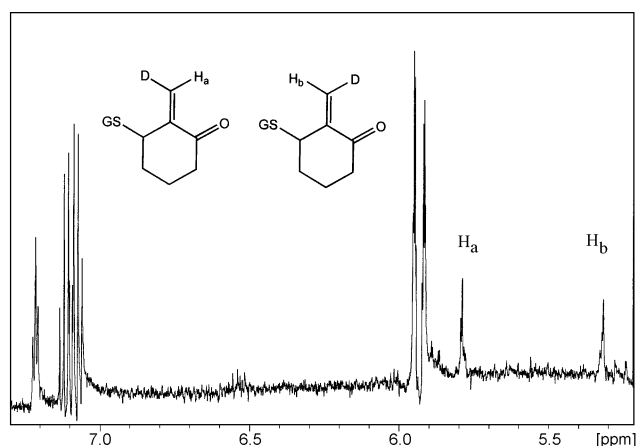


**Figure 6.** Vinyl region in the <sup>1</sup>H NMR spectrum (500 MHz, D<sub>2</sub>O, ref HOD; solvent suppression applied) of a reaction mixture composed of hGSTP1-1 (1.7 units), (S)d<sub>1</sub>-1b (0.83 mM), GSH (0.17 mM) and potassium phosphate buffer (33 mM) in D<sub>2</sub>O, pD 6.5, 21 °C. The reaction mixture (0.6 mL) was stopped after 10 min incubation by the addition of trichloroacetic acid to 2% final concentration and extracted with CDCl<sub>3</sub> to remove excess COMC-6 before analysis. The exomethylene protons H<sub>a</sub> and H<sub>b</sub> occur at δ 5.79 and δ 5.32, respectively. The triplet at δ 7.22 corresponds to the endocyclic vinyl proton resonance of 2b; the multiplets at δ 7.10 and 5.93 are due to the vinyl protons of crotonic acid.

(stereospecifically labeled with deuterium at the exomethylene carbon) was incubated in the presence of high concentrations of hGSTP1-1. The resultant exocyclic enone was rapidly trapped in acid solution, and the ratio of the *Z* and *E* isomers was determined by <sup>1</sup>H NMR spectroscopy, as detailed in the legend to Figure 6. We reasoned that if conversion of the putative glutathionylated enol(ate) to the exocyclic enone takes place in the asymmetric environment of the active site, either the *Z* or *E* isomer of product would predominate, depending on whether the preferred conformation of the enzyme-bound enol(ate) involves a syn or anti relationship between the crotonate-leaving group and the GS moiety (e.g., Scheme 5).

Alternatively, if the active site does not exert strict stereochemical control over the elimination reaction or if elimination takes place after dissociation of the enol(ate) from the active site (Scheme 6), similar (although not necessarily equal) amounts of the *Z* and *E* isomers would be expected.

The deuterium-labeled substrates (R)d<sub>1</sub>-1b and (S)d<sub>3</sub>-1b were prepared by using HLADH to stereospecifically introduce different isotopes of hydrogen at the pro-*R* position of the exomethylene function of 5b, followed by crotonylation of the labeled alcohol (Experimental Section). Using either (S)d<sub>3</sub>-1b or (R)d<sub>1</sub>-1b as substrates for hGSTP1-1 under conditions where >80% of the substrate is processed by the enzyme, we found that the ratio of the integrated intensities of the upfield versus downfield resonances of the geminal vinylic hydrogens of the isolated exocyclic enone was 0.89 ± 0.09 and 1.01 ± 0.1, respectively (e.g., Figure 6).

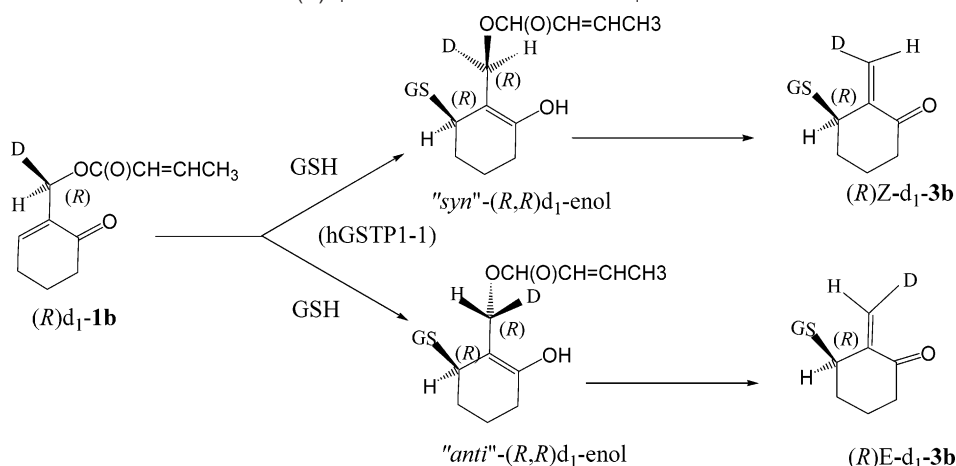
A similar ratio was obtained (1.05 ± 0.11) under conditions where the reaction mixture contained a 5-fold excess of GSH over (R)d<sub>1</sub>-1b. The fact that stereorandomly D-labeled exocyclic enone is observed independent of the concentration of GSH in the reaction mixture argues against equilibration of the *Z* and *E* stereoisomers after their formation by the enzyme. Thus, the results indicate the absence of strict stereochemical control over the conversion of the glutathionylated enol(ate) to the exocyclic enone.

**Isozyme Specificity for COMC-6.** To evaluate isozyme specificity, the steady-state kinetic constants of COMC-6 with different enzyme variants of the *alpha*, *mu*, *pi*, and *theta* class GSTs were determined (Table 3).<sup>15</sup>

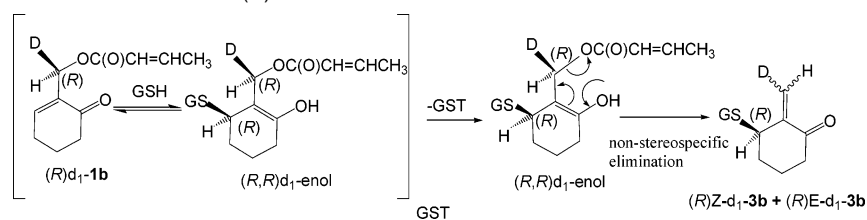
Enzyme assays were carried out under conditions where the enzyme-catalyzed step is completely rate-limiting (see Experimental Section). The  $k_{cat}$  and  $k_{cat}/K_m$  values for COMC-6 with the *alpha*, *pi*, and *mu* class enzymes are within a factor of 4 of one another. The  $k_{cat}$  values for COMC-6 and ethacrynic acid differ by a factor of about 4 using the recombinant hGSTP1-1 isoform. This is the smallest difference found for these two substrates among all of the GSTs tested. In addition, human placental hGSTP1-1, composed of the V105 and I105 variants,<sup>16</sup> was also found to catalyze the conversion of COMC-6 to GSMC-6 with kinetic constants ( $k_{cat} = 1.2 \pm 0.2 \text{ s}^{-1}$ ,  $K_m = 0.052 \pm 0.010 \text{ mM}$ ) similar in magnitude to those obtained with ethacrynic acid ( $k_{cat} = 1.0 \pm 0.03 \text{ s}^{-1}$ ,  $K_m = 0.034 \pm 0.007 \text{ mM}$ ) under the same assay conditions (1 mM GSH, pH 6.5, 25 °C). In contrast, there are significant differences in the efficiencies with which COMC-6 and ethacrynic acid are processed by the *alpha* and *mu* class enzymes. The  $k_{cat}$  values for COMC-6 are about 35-fold and about 70-fold larger than those for ethacrynic acid with hGSTA1-1 and hGSTM2-2, respectively. The *theta* class rGSTT2-2 shows no activity with either COMC-6 or ethacrynic acid.

**Molecular Docking Studies.** Docking studies were undertaken in an attempt to identify possible catalytic residues in the active site that could promote the Michael addition reaction between GSH and COMC-6. The AutoDock 3.0 program was used<sup>14</sup> because preliminary experiments showed that this program could very precisely reproduce the protein–ligand interactions observed in the X-ray crystal structure of the GS–

- (15) (a) Mannervik, B.; Awasthi, Y. C.; Board, P. G.; Hayes, J. D.; Dillio, C.; Ketterer, B.; Listowsky, L.; Morgenstern, R.; Muramatsu, M.; Pearson, W. R.; Pickett, C. B.; Sato, K.; Widersten, M. *Biochem. J.* **1992**, *282*, 305–306. (b) Montali, J. A.; Wheatley, J. B.; Schmidt, D. E., Jr. *Cell. Pharmacol.* **1995**, *2*, 241. (c) Kauvar, L. M. In *Structure and Function of Glutathionyl Transferases*; Tew, K., Pickett, C., Mantle, T., Mannervik, B., Hayes, J., Eds.; CRC Press: Boca Raton, FL, 1993; p 251.
- (16) (a) Zimniak, P.; Nanduri, B.; Pikula, S.; Bendorowicz-Pikula, J.; Singhal, S.; Srivastava, S. K.; Awasthi, S.; Awasthi, Y. C. *Eur. J. Biochem.* **1994**, *224*, 893–899. (b) Johansson, A. S.; Stenberg, G.; Widersten, M.; Mannervik, B. *J. Mol. Biol.* **1998**, *278*, 687–698.

**Scheme 5.** Possible Stereochemical Routes from (*R*)*d*<sub>1</sub>-**1b** to the *Z* or *E* Isomers of *d*<sub>1</sub>-**3b** in the Active Site of hGSTP1-1<sup>a</sup>

<sup>a</sup> The chirality of the glutathionylated carbon is assumed to be *R*, consistent with the results of molecular docking studies described below.

**Scheme 6.** Possible Stereochemical Route from (*R*)*d*<sub>1</sub>-**1b** to a Mixture of *Z* and *E* Isomers of *d*<sub>1</sub>-**3b****Table 3.** Steady-State Kinetic Constants for COMC-6 with Different Classes of Recombinant Glutathione Transferase (GST)<sup>a</sup>

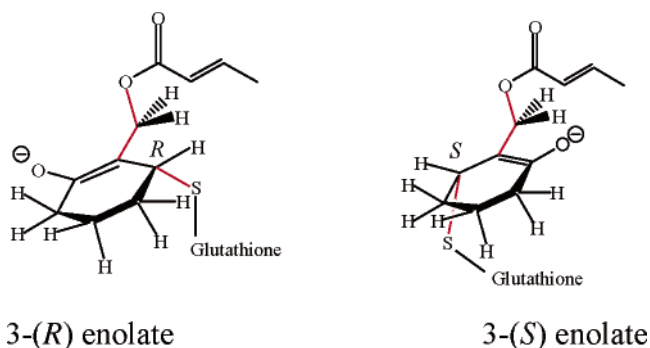
class (variant)	$k_{cat}$ , min <sup>-1</sup>	$K_m$ , mM	$(k_{cat}/K_m) \times 10^{-3}$ , mM <sup>-1</sup> min <sup>-1</sup>	[COMC-6] range, mM
<i>alpha</i> (hGSTA1-1)	90 ± 12	0.13 ± 0.03	0.72 ± 0.12	0.025–0.280
<i>alpha</i> (hGSTA4-4)	<i>c</i>	<i>c</i>	2.76 ± 0.36	0.013–0.280
<i>pi</i> (hGSTP1-1)	138 ± 12	0.08 ± 0.01	1.80 ± 0.18	0.013–0.150
<i>mu</i> (hGSTM2-2)	366 ± 48	0.34 ± 0.07	1.08 ± 0.08	0.013–0.280
<i>theta</i> (rGSTT2-2)	ND	ND	ND	0.1

<sup>a</sup> Conditions: GSH (1 mM), sodium phosphate (0.1 M, pH 6.5), 30 °C,  $\Delta\epsilon_{235} = -2400 \text{ M}^{-1} \text{ cm}^{-1}$ . <sup>b</sup>  $k_{cat}$  values for ethacrynic acid (EA) estimated from published specific activities and subunit molecular weights.<sup>8</sup> <sup>c</sup> Saturation not achieved. <sup>d</sup> ND, no detectable activity (<0.05  $\mu\text{mol min}^{-1} \text{ mg}^{-1}$  at 0.1 mM COMC-6).

EA conjugate in the active site of hGSTP1-1 (PDB code 3GSS).<sup>17</sup> Thus, the program should give useful information about the most stable conformations of similar GSH adducts in the active site of hGSTP1-1.

Docking experiments were carried out using the two hypothetical diastereomeric enolates, which would form from the addition of GSH to the *2*si*-3*re** face or to the *2*re*-3*si** face of COMC-6 (Chart 2).

The diastereomers were first constructed and optimized in Macromodel 7.1 except for the glutathionyl group, which was taken from the crystal structure and kept rigid during docking. The optimized structures were then docked into the active site of 3GSS, allowing only the three bonds highlighted in red to

**Chart 2**

rotate (Chart 2). The binary complex with the 3-(*R*) enolate was found to be about 1 kcal/mol more stable than that with the 3-(*S*) diastereomer (Figure 7).

Both complexes suggest catalytic roles for the active site Tyr108 and Tyr7 residues, as discussed below.

## Discussion

This work has clarified several aspects of the basic enzyme chemistry associated with the conjugation of GSH with the COMC derivatives, which might provide a basis for understanding their tumoricidal activities.

**Minimum Kinetic Mechanism.** The kinetic measurements and stereochemical studies suggest that the processing of the COMC derivatives by GST involves initial enzyme-catalyzed Michael addition of GSH to the COMC derivative to give a glutathionylated enol(ate), which undergoes stereorandom loss of crotonate, while either bound to the active site or free in solution, to give a glutathionylated exocyclic enone (Schemes 5 and 6). Once free in solution, GSH reacts at the exomethylene carbon of the exocyclic enone, displacing the first GSH to give

(17) (a) Oakley, A. J.; Rossjohn, J.; Lo Bello, M.; Caccuri, A. M.; Federici, G.; Parker, M. W. *Biochemistry* **1997**, *36*, 576–585. (b) Lo Bello, M.; Oakley, A. J.; Battistoni, A.; Mazzetti, A. P.; Muccetelli, M.; Mazzaresse, G.; Rossjohn, J.; Parker, M. W.; Ricci, G. *Biochemistry* **1997**, *36*, 6207–6217.



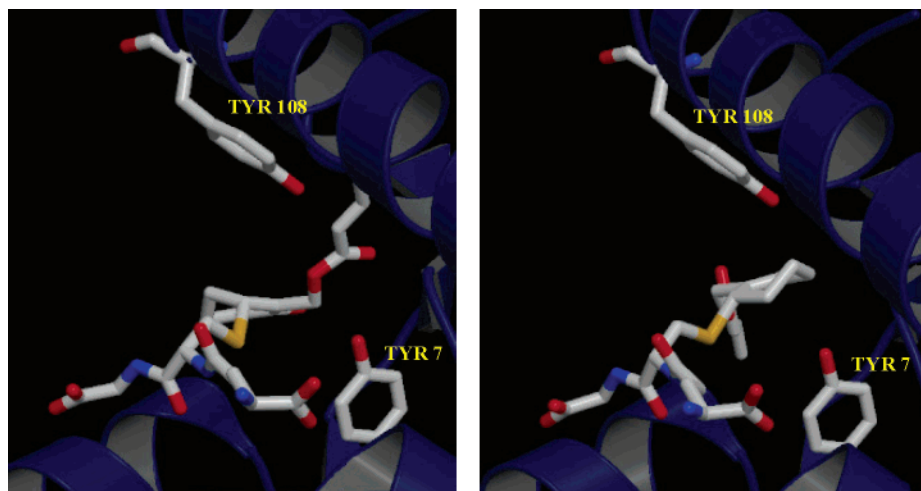


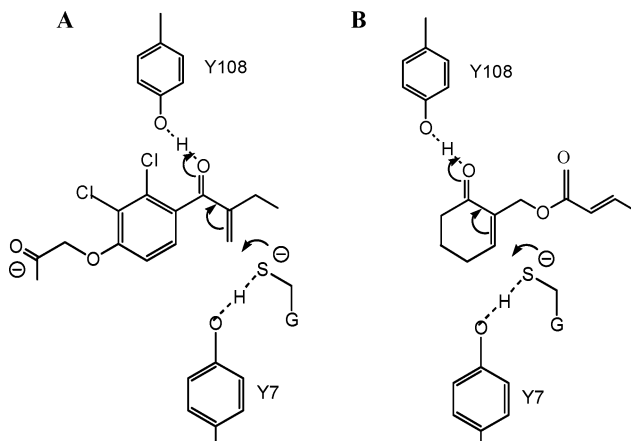
**Figure 7.** Lowest-energy binding modes of the 3-(*R*) (left panel) and 3-(*S*) (right panel) diastereomers of the enolate shown in Chart 2 bound to the active site of 3GSS.

the final product (Scheme 2). Apparently, all three COMC derivatives are processed by the same reaction mechanism, as they all exhibit similar kinetic profiles and kinetically competent exocyclic enones were successfully isolated from reaction mixtures containing either COMC-6 or COMC-7 as substrates. The above mechanism is in sharp contrast to that proposed by previous workers who believed that the conjugation of GSH with COTC and COMC-6 involved a simple in-line displacement mechanism leading directly to the GSH conjugate.<sup>4</sup> Certainly, in the absence of GST there is a smooth, first-order conversion of the COMC derivatives to the final GSH adduct, showing no evidence of an intermediate species (Figures 2 and 4). Since the initial conjugation reaction is rate-determining, the formation of the exocyclic enone could not be detected kinetically (Table 1). However, in the presence of high concentrations of GST, the multiphase nature of the reaction is apparent, indicating the formation of a reactive intermediate prior to formation of the final product. Conceivably, the enzymatic reaction might go by a multistep mechanism while the nonenzymatic reaction involves an in-line displacement mechanism. However, this seems unlikely, as glutathionylated enols have been detected by mass spectrometry in nonenzymatic reaction mixtures containing excess COMC-6 over GSH.<sup>6</sup>

The catalytic rate enhancements ( $(k_{\text{cat}}/K_m)/k_1$ ) for the enzymatic processing of COMC-5, COMC-6, and COMC-7 are modest but significant, corresponding to values of  $1.0 \times 10^4$ ,  $2.1 \times 10^4$ , and  $6.7 \times 10^4$ , respectively (Tables 1 and 2). Enzymatic catalysis is probably not limited by chemistry alone. The nonenzymatic rate constants for formation of the exocyclic enones from COMC-5, COMC-6, and COMC-7 progressively decrease in magnitude with increasing ring size. This trend could reflect progressively poorer orbital overlap between the carbon-carbon double bond and the conjugated carbonyl group in the transition state due to increasing “ring pucker” with increasing ring size. However, this trend is not reflected in a significant change in  $k_{\text{cat}}/K_m$  for the COMCs with hGSTP1-1, possibly because catalysis is limited by a conformational transition or product release from the active site.

**Catalytic Mechanism.** The mechanism by which hGSTP1-1 catalyzes the initial Michael addition reaction between GSH and COMC-6 is probably fundamentally similar to that previously

**Chart 3.** Possible Catalytic Mechanism for the Glutathione Transferase-Catalyzed Michael Addition of GSH to (A) Ethacrynic Acid (EA) and to (B) COMC-6



proposed for the catalyzed addition of GSH to EA.<sup>17</sup> The X-ray crystal structure of hGSTP1-1 in complex with the GS–EA adduct suggests that the hydroxyl group of Tyr108 functions as a general acid catalyst by interacting with the carbonyl group of the enone function of EA during the addition reaction with GSH (Chart 3).

Moreover, the hydroxyl group of Tyr7 is in close proximity to the sulfur atom of bound GS–EA and, by inference, probably stabilizes (via H-bonding) the nucleophilic mercaptide anion form of bound GSH prior to reaction.<sup>18</sup> The molecular docking studies reported here suggest that the glutathionylated enolate derived from COMC-6 binds to the active site in a fashion similar to that of GS–EA observed in the X-ray crystal structure (Figure 7). By inference, the OH group of Tyr108 is well-positioned to function as a general acid catalyst by interacting with the carbonyl group of the enone function of COMC-6 in the transition state, and the hydroxyl group of Tyr7 is positioned to stabilize the mercaptide ion form of GSH. Thus, a common catalytic mechanism can be envisioned for EA and COMC-6.

This mechanism also comports with the observation that COMC-6 and EA are both substrates for the *alpha*, *mu*, and *pi*

(18) Armstrong, R. N. *Chem. Res. Toxicol.* **1997**, *10*, 2–18.

class variants of GST (Table 3). All three classes of GST are capable of catalyzing the same general type of chemistry, as their active sites contain functional groups analogous in position to those observed in the crystal structure of hGSTP1-1. This conclusion is based on a large number of sequence alignments, structural comparisons, and site-directed mutagenesis studies of the major GST isoforms, extensively reviewed elsewhere.<sup>18,19</sup> The explanation for why the recombinant *theta* class enzyme rGSTT2-2 does not use EA or COMC-6 as a substrate is unclear (Table 3). The *theta* class GSTs show only about 7% sequence homology with the *alpha*, *mu*, and *pi* class enzymes, and the functional groups in the active site have not been completely identified.<sup>8e,20</sup> The preponderance of the evidence, therefore, suggests that general acid catalysis plays a key role in the Michael addition reactions between GSH and the COMC derivatives catalyzed by all three major classes of GST.

What happens immediately after formation of the glutathionylated enol(ate) in the active site is less clear. Stereorandom loss of crotonate from the intermediate implies that elimination takes place in bulk solvent after dissociation of the intermediate from the active site (Scheme 6). This type of argument has often been used to rationalize nonstereospecific steps in metabolic processes. Nevertheless, there is no absolute assurance that the structural features of the active site of GST will constrain the elimination step to follow only one of the stereochemical routes shown in Scheme 5, particularly in view of reports that some isozymes of GST can nonstereospecifically process substrates. For example, the rGSTM2-2 isozyme reportedly catalyzes the addition of GSH to 4-phenyl-3-buten-2-one with a high degree of stereoselectivity (90%).<sup>21</sup> In contrast, the M1-1 isozyme catalyzes the very same reaction with little stereoselectivity. In view of these observations, the stereorandom elimination of crotonate from the glutathionylated enol(ate) might still be an active-site process subject to enzymatic catalysis.

**What Is the Chemical Basis of Antitumor Activity?** The studies described here were originally motivated by an interest in the mechanism by which COTC and COMC-6 inhibit tumor growth (Scheme 1). Tumoricidal activity was once thought to arise from inhibition of the methylglyoxal-detoxifying enzyme glyoxalase I by the GSH adducts formed with COTC and COMC-6.<sup>4</sup> However, recent studies show that the adducts are poor competitive inhibitors of human glyoxalase I.<sup>1,5</sup> Even more importantly, the diethyl ester prodrug form of the GSH conjugate GSMC-6 was found not to have significant antitumor activity with B16 melanotic melanoma in vitro ( $IC_{50} > 460 \mu M$ ) versus COMC-6 ( $IC_{50}$  0.046  $\mu M$ ) and the five- and seven-membered-ring homologues COMC-5 ( $IC_{50}$  0.144  $\mu M$ ) and COMC-7 ( $IC_{50}$  0.029  $\mu M$ ).<sup>2</sup> Therefore, tumoricidal activity cannot be due to the final GSH conjugate GSMC-6, but must result directly from COMC-6 and/or from an intermediate species formed during its conjugation with GSH. Preliminary studies indicating that the conjugation reaction is indeed a multistep process involving the intermediate formation of an electrophilic exocyclic enone led to the current hypothesis that tumor toxicity might reflect, in part, the ability of exocyclic enone to alkylate biomacromolecules vital to cell function.<sup>1</sup>

The detailed kinetic work described here strongly indicates that all three cytotoxic COMC derivatives react with GSH via mechanisms involving the formation of electrophilic exocyclic enones, implying that the cytotoxicity of the COMC derivatives has a common mechanistic explanation. The fact that the exocyclic enones are better Michael acceptors than the unmodified COMCs (Table 1) suggests that the exocyclic enones might be the actual toxic species in tumor cells, at least from a simple chemical perspective. Nevertheless, the unmodified COMCs are also good Michael acceptors and more work is needed before any final conclusions can be reached with respect to the relative cytotoxicities of the COMCs and their exocyclic enones in highly compartmentalized tumor cells. Whatever the specific chemical identity of the cytotoxic species inside tumor cells, cell death could result from genotoxicity. This follows from the observation that COMC-6 forms covalent adducts with the exocyclic amino groups of the nucleotide bases composing single-stranded oligonucleotides in cell-free systems, either in the presence or in the absence of GSH.<sup>6</sup>

**What Is the Role of GST in Antitumor Activity?** All human tissues contain GST activity, which is usually differentially distributed among different isozymes of GST based on tissue type.<sup>22</sup> The *pi* class of GST is of particular interest from a chemotherapeutic perspective, as it is often overexpressed in tumor tissue versus normal tissue. GSTs are thought to detoxify antitumor drugs by catalyzing their conversion to GSH-drug conjugates, which are subsequently removed from cells by a membrane-associated protein pump. Repeated exposure to antitumor agents often leads to even greater expression of GST activity in tumor cells and the development of multidrug resistance (MDR).<sup>7</sup> For example, MCF7 human breast cancer cell lines, which have been selected for resistance to different types of antitumor agents, can overexpress the *pi* GST isozyme at levels 10-fold greater than that observed in the wild-type tumor cell line. Overcoming MDR is one of the major unmet challenges facing medicinal enzymology.

GST undoubtedly plays an important role in the metabolism of the COMC derivatives in some types of cells. The fraction ( $F$ ) of COMC derivative undergoing enzymatic versus nonenzymatic conversion to GSH conjugate is formally given by

$$F = \frac{\sum (V_{\max}/K_m^{\text{COMC}})}{k_1[\text{GSH}] + \sum (V_{\max}/K_m^{\text{COMC}})} \quad (1)$$

where  $\sum (V_{\max}/K_m^{\text{COMC}})$  equals the sum of the  $V_{\max}/K_m^{\text{COMC}}$  activities of the different GST isozymes and  $k_1[\text{GSH}]$  is the apparent rate constant for the nonenzymatic formation of GSH conjugate. This equation applies under the most likely physiological conditions, where  $[\text{GSH}]$  equals about 5 mM and therefore is  $\gg K_m^{\text{GSH}}$  ( $\sim 0.2$  mM),<sup>7</sup> and  $[\text{COMC}] \ll K_m^{\text{COMC}}$ . From published enzyme activities,<sup>23</sup> wild-type MCF7 cells are estimated to contain 0.21 CDNB units of hGSTP1-1 activity/mL cell cytosol. This translates into about 0.011 COMC-6 units/mL cytosol, using the published activities hGSTP1-1 with CDNB versus EA<sup>7</sup> and the activities of hGSTP1-1 with EA

(19) (a) Mannervik, B.; Danielson, U. H. *Crit. Rev. Biochem. Mol. Biol.* **1988**, *23*, 283–337. (b) Daniel, V. *Crit. Rev. Biochem. Mol. Biol.* **1993**, *28*, 173–207. (c) Wilce, M. C. *Biochim. Biophys. Acta* **1994**, *1205*, 1–18. (d) Dirr, H.; Reinemer, P.; Huber, R. *Eur. J. Biochem.* **1994**, *220*, 645–661. (20) Pemble, S. E.; Taylor, J. B. *Biochem. J.* **1992**, *287*, 957–963. (21) Chen, J.; Armstrong, R. N. *Chem. Res. Toxicol.* **1995**, *8*, 580–585.

(22) Johansson, A.-S.; Mannervik, B. In *Interindividual Variability in Human Drug Metabolism*; Pacifici, G. M., Pelkonen, O., Eds; Taylor and Francis: London, 2001; pp 460–519.

(23) Morrow, C. S.; Smitherman, P. K.; Diah, S. K.; Schneider, E.; Townsend, A. J. *J. Biol. Chem.* **1998**, *273*, 20114–20120.

versus COMC-6 (Table 3). This activity and the  $k_1$  and  $K_m^{\text{COMC}}$  values given in Tables 1 and 2 with eq 1 indicates that about 40% of the COMC-6 is processed by hGSTP1-1 in wild-type MCF7 cells. For MDR cells that overexpress hGSTP1-1 by greater than 10-fold, the fraction processed by the enzyme is greater than 87%. A similar analysis for COMC-7 indicates that in wild-type MCF7 versus MDR MCF7 cells, the fractions processed by the enzyme are 70% and >96%, respectively. Therefore, hGSTP1-1 is probably responsible for processing a significant fraction of COMC-6 and COMC-7 in both wild-type and MDR MCF7 cells.

From the standpoint of tumor toxicity, overexpression of GST activity could have the following consequences, assuming that a steady-state kinetic model applies in which the rate of influx of COMC derivative into tumor cells is equal to the rate of conversion to GSH conjugate (Scheme 2). First, if the unmodified COMC derivative is directly responsible for tumoricidal activity, overexpression of GST activity could protect tumor cells from cytotoxicity by lowering the steady-state concentration of intracellular COMC derivative and, therefore, decreasing the rate of covalent modification of vital biomacromolecules. Second, if the COMC derivative and the exocyclic enone are equally toxic to tumor cells, overexpression of GST would have little effect on cytotoxicity. In this case, the COMC derivatives should be exceptionally resistant to the development of MDR. Third, if the exocyclic enone is primarily responsible for anti-tumor activity, overexpression of GST activity would actually increase the sensitivity of tumor cells to the COMC derivative by increasing the steady-state concentration of the exocyclic enone. Thus, tumor-selective toxicity would be a function of the ratio of the rates of formation of the exocyclic enone in MDR cells that overexpress GST versus normal cells that express lower levels of GST (eq 2).

$$\frac{[\text{exo}]_{\text{MDR}}}{[\text{exo}]_{\text{normal}}} = \frac{k_1[\text{GSH}] + \sum (V_{\text{max}}/K_m^{\text{COMC}})_{\text{MDR}}}{k_1[\text{GSH}] + \sum (V_{\text{max}}/K_m^{\text{COMC}})_{\text{normal}}} \quad (2)$$

This ratio will be maximal (and differential toxicity greatest) when the enzymatic rate of formation of the exocyclic enone greatly exceeds the nonenzymatic rate ( $k_1[\text{GSH}] \ll \sum (V_{\text{max}}/K_m^{\text{COMC}})$ ). Under these conditions,  $[\text{exo}]_{\text{MDR}}/[\text{exo}]_{\text{normal}}$  approaches the ratio of total GST activity in MDR tumor cells versus normal cells.

### Summary

The work reported here demonstrates that the GST-catalyzed conversion of COMC derivatives to the corresponding GSH conjugates is a multistep process involving the formation of a highly reactive glutathionylated exocyclic enone. Thus, the antitumor activities of the COMC derivatives might be explained on the basis of the ability of the exocyclic enone and/or underivatized COMC to function as Michael acceptors, resulting in the alkylation of biomacromolecules critical to cell viability. Finally, the differential expression of GST activity between normal cells and tumor cells could have a major influence on the differential toxicity of COMC derivatives to tumor cells.

**Acknowledgment.** We thank the University of Maryland, College of Life Sciences for MS and the UMBC Center for Structural Biochemistry for NMR spectra. This work was supported by grants from the NIH (CA 59612 to D.J.C.; GM 24054 to B.G.; GM 61402 to K.N.H.), the U.S. Army Medical Research and Material Command (DAMD17-99-1-9275 to D.J.C.), and the Swedish Cancer Society (to B.M.).

JA030396P